

## Effective Adsorption of Fe<sup>2+</sup> and Pb<sup>2+</sup> Ions from Polluted groundwater Using Moringa Seeds (Case Study: El-Sadat Area, Egypt)

Ehab Zaghlool and Mohamed E.A. Ali

Hydrogeochemistry Department & Egypt Desalination Research Center of Excellence (EDRC), Desert Research Center, Cairo, 11753, Egypt

Received: 28 March 2020 / Accepted 30 May 2020 / Publication date: 20 June 2020

### ABSTRACT

This study examined the removal of heavy metal ions with takes in the consideration of (Fe<sup>2+</sup> and Pb<sup>2+</sup>) from aqueous solutions and/or groundwater by adsorption technique using Moringa seeds. The groundwater quality indicators including total dissolved salts (TDS), ion ratios, and indices of the studied area for heavy metals contamination were examined. TDS values show 80% of groundwater samples being fresh while the rest are brackish. To identify the source of groundwater contamination either seepage of fertilizer, septic tank leakage, sewage or natural deposition erosion and hydrochemical ratios of the collected groundwater samples were considered. Based on heavy metal pollution index, 36% of groundwater samples were classified as poor samples, 60% as very poor and 4% were unsuitable samples. Additionally, 24 % of groundwater samples were found to be contaminated with Fe<sup>2+</sup>, while all samples are contaminated with Pb<sup>2+</sup>. The possibility of using moringa seeds for adsorption or removal the toxic ions from water was carried out. The removal efficiency of the Fe<sup>2+</sup> and Pb<sup>2+</sup> ions were found to surpass 90%. It was concluded that adsorption of Fe<sup>2+</sup> was fitted better to Freundlich model than the Langmuir, and vice versa in case of Pb<sup>2+</sup>.

**Keywords:** Groundwater, Heavy Metal ions, Moringa Seeds, Adsorption

### Introduction

Groundwater quality deterioration is one of the main problems facing all over the world, fresh groundwater contributes to less than 20% of the total potential of water resources in Egypt (Allam *et al.*, 2003). Currently, the renewable water resources decrease from 2189 m<sup>3</sup>/capita/year in 1966 to 670 m<sup>3</sup>/capita/year in 2013 (Abdel-Shafy and Mansour, 2013). These challenges urge governments to find new approaches to provide water such as desalination, wastewater treatment, and management the groundwater resources. Despite groundwater considers the easiest way to provide water, unfortunately it has been affected by pollution because of human activities, industrial seepage from drainages around the industrial zones or through natural constituents of the earth's crust. In this manner, several studies showed that groundwater in some areas had high concentrations of the trace elements in the western Nile delta aquifers such as iron, manganese and nickel (Sharaky *et al.*, 2007; Agrama, and El-Sayed, 2013). Nowadays major problem in the global context is the pollution of groundwater by heavy metals, which considers one of the most harmful of the chemical pollutants because of their toxicities to humans. The removal of these heavy metals from groundwater is essential before it can be discharged for human use. The most conventional techniques for wastewater treatment are chemical precipitation, redox reactions, Electrodialysis, and filtration membranes (Gupta *et al.*, 2010, Najafabadi, 2015, Piedra *et al.*, 2015). Inappropriately, all or some of those methods need sophisticated equipment and high cost. Lately, many researchers portrayed that using the natural products for water treatment has economic value, safe, and environmentally friendly (Glenda and Gregory, 1996; Annadurai *et al.*, 2003; Singh *et al.*, 2006; Alinnor, 2007; Fu and Wang, 2011). One of the common plants have been used in this manner is *Moringa oleifera* seeds, which have good biosorption properties of heavy metals and in the same time act as coagulant for turbidity from surface water (Reddy *et al.*, 2010 and 2012; Veronica *et al.*, 2012). Usually, *Moringa oleifera* grows in tropical regions, and their seeds and leaves have been used in water treatment on small scale in some African countries. Previous studies revealed that the carboxylic and amino groups included in the chemical structure of the moringa seeds act as active sites for adsorption or even reaction with heavy metals (Obuseng *et al.*, 2012; Irene *et al.*, 2016). Others concluded that heavy metal adsorption mechanism occurs only on the surface, this is because moringa contains a low

**Corresponding Author:** Ehab Zaghlool, Hydrogeochemistry Department & Egypt Desalination Research Center of Excellence (EDRC) Desert Research Center, Cairo, 11753, Egypt  
E-mail: ezaghlooldrc@yahoo.com

molecular weight short chains acting as cationic polyelectrolyte. The adsorption of heavy metals ensues through formation a bridge and/or a complex between their positive charges and negatively charged (lone pair of electrons) of the moringa protein molecules.

The purpose of this study was to detect the pollution of groundwater of El-Sadat area by heavy metals, in addition, using moringa seeds for removal of some heavy metals from aqueous solution by adsorption. The optimum dose, pH, and isotherm studies of iron and lead ions using moringa seeds were investigated.

### Description of the study area.

El-Sadat city locates in the western desert of Egypt, bounded by longitudes 30.4° and 30.7° E and latitudes 30.3° and 30.6° N, (Fig. 1). Great efforts have being paid by governmental and non-governmental organization to sustain natural resources to maintain the sustainability of agricultural and industrial projects in the area under investigation. In the study area the groundwater considered the main source for agricultural activities suffering from groundwater table depletion due to over pumping (Ghaly, 2001) and the influence of the infiltration of the wastewater ponds that received domestic and industrial wastewater from El-Sadat city.

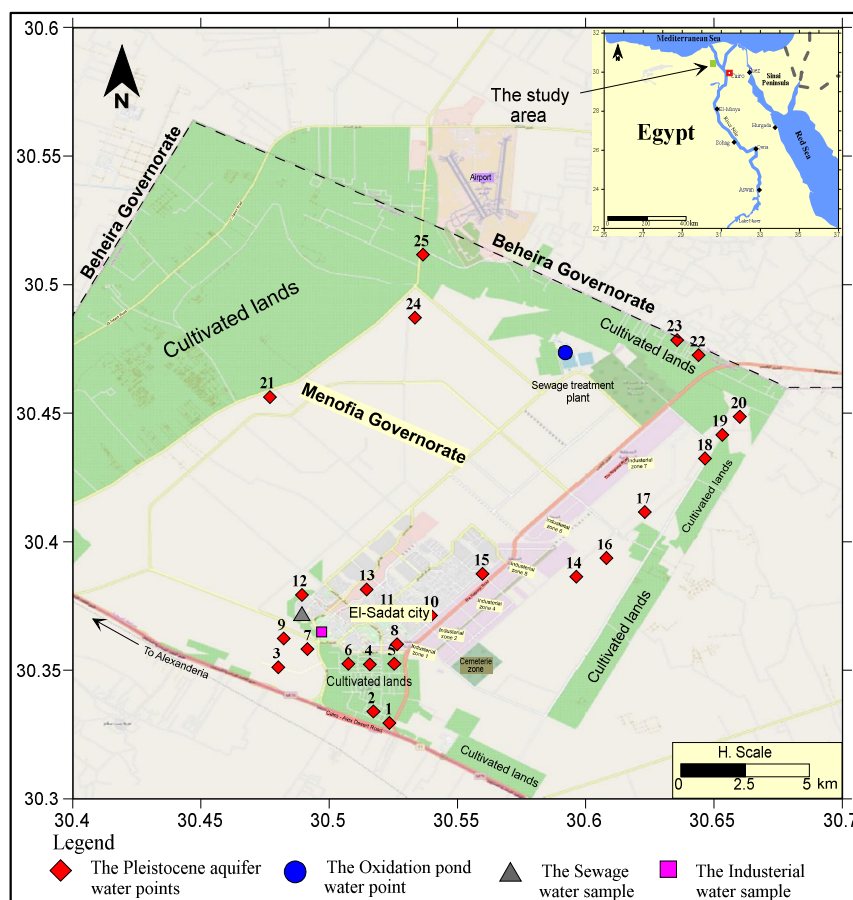


Fig. 1: Location and well location map of the study area.

The study area is characterized by old alluvial plain units of the north and east of Wadi E1-Natron area with elevations vary from 20 m in the east to 70 m in the west near Wadi E1-Natron, covered by Quaternary sediments composed mainly of sand, gravel with clay pockets (Kenawy *et al.*, 2016). The Pleistocene aquifer is the main productive formation consists of sand and gravels intercalated with clay lenses (Al-Kilany, 2001). The bottom of the aquifer bounded by a thick section of Pliocene clay (Menco, 1990), the aquifer thickens decrease from 300 m at the North eastern portion to 80 m near to Cairo – Alexandria desert road, the flow direction of the Pleistocene groundwater is from the northeast to the

southwest toward Wadi El-Natron depression (Ahmed *et al.*, 2011) (Fig. 2). The Pleistocene aquifer in the study area is unconfined and semi-confined in the north eastern portion in the study area where the clay cap covers the aquifer, the groundwater level ranged from 8 m in the north eastern part to 20 m near the Cairo – Alexandria desert road (Ahmed *et al.*, 2011). The Pleistocene aquifer in the study area is recharged from the groundwater basin underlying the Nile delta which is built of the same Pleistocene formations (Abd El-Baki, 1983) and by lateral seepage from the irrigation canals (Ahmed *et al.*, 2011).

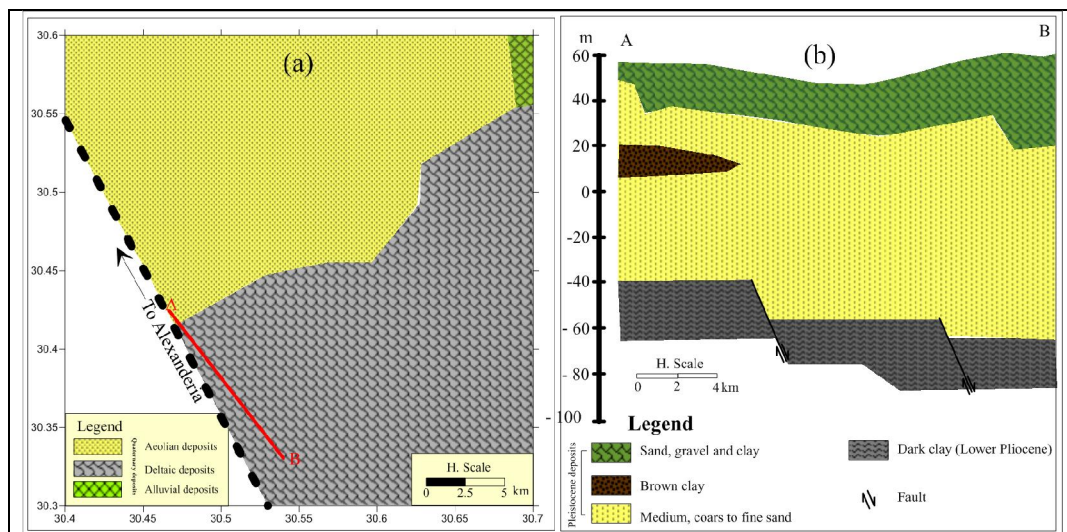


Fig. 2: a) Geologic Map of the Study Area (CONOCO, 1987) b) Geological cross section A–B (El-Sayed, 1999).

**Experimental**

**Sampling and water analysis**

Groundwater samples were collected from 25 water wells tapping to the Pleistocene aquifer and 3 water samples represents the oxidation pond (O.P), domestic sewage water (D.S) and industrial sewage (I.S), all water samples were collected from the study area during January 2019, (Fig. 1). The samples were collected in 1-liter pre-cleaned polypropylene bottles for ions measurements. 50 ml of water samples were preserved by acidifying to pH < 2 with HNO<sub>3</sub> in a 50 ml pre-cleaned polypropylene bottles. PH and electrical conductivity (EC) were measured in during the field trip using Orion portable meters. Sodium, Potassium, Chloride, Sulphate, Nitrate, Ammonia and Bromide ions were measured using ion chromatography system (Dionex, ICS-1100). Heavy metals were measured by using inductive coupled plasma mass spectrometry (ICP, POEMSIII, thermo Jarrell elemental company USA).

**Pollution indices:**

**a- Heavy metal pollution index:**

Heavy metal pollution index, HPI is a comprehensive tool used for overall water quality determination, according to calculated weights of each metal (Horton, 1965; Mohan *et al.*, 1996), HPI was calculated according to the following equation:

$$HPI = \frac{\sum_{i=1}^n WiQi}{\sum_{i=1}^n Wi}$$

Wi is the unit weightage of the heavy metal (i), n is the number of heavy metals  
 Qi is the sub-index of the heavy metal.

$$Wi = k/Si$$

K is the proportionality constant; Si is the standard permissible limit of the heavy metal.

$$K = \frac{1}{\sum_{i=1}^n S_i} \quad \sum_{i=1}^n \frac{1}{S_i} = \frac{1}{S_1} + \frac{1}{S_2} + \dots \dots \dots \frac{1}{S_i}$$

Where,  $S_1, S_2, S_3,$  and  $S_i$  represent standards for different heavy metals in the groundwater samples.

$$Q_i = 100 \times (V_i/S_i)$$

$V_i$  is the monitored value of the  $i$  parameter in mg/l, HPI is classified into five classes, excellent (0–25), good (26–50), poor (51–75), very poor (76–100) and unsuitable (100).

#### b- Nitrate pollution index:

Nitrate sources in the groundwater are classified to point sources such as irrigation of land by sewage effluents and nonpoint sources such as unsewered sanitation in densely populated area and intensive agricultural activities (McLay *et al.*, 2001). The NPI for the water samples was calculated by using the following relation:

$$NPI = (C_s - HAV) / HAV$$

Where  $C_s$ : The analytical concentration of nitrate

HAV: The threshold value of anthropogenic source (human affected value) taken as 20 mg/L (Spalding and Exner, 1993).

The water quality according to NPI values was classified into five types: clean (unpolluted)( $NPI < 0$ ), light pollution ( $0 < NPI < 1$ ), moderate pollution ( $1 < NPI < 2$ ), significant pollution ( $2 < NPI < 3$ ), very significant pollution ( $NPI > 3$ ).

#### Collection and refining of Moringa Seeds

Dry moringa seeds were obtained a farm in north Sinai and stored at room temperature prior to use, the seeds were unshelled, and the kernels were washed with plentiful amounts of deionized water to remove any sticking dirt before drying in the oven at 65 °C for 24 h. The dried samples were grounded and sieved to obtain a fine powder of 0.63 μm mesh size. The oil was extracted by soxhlet extraction using as follow; About 176 g of grounded moringa seeds and copious volume of petroleum ether were put into a soxhlet extraction apparatus. The weight of oil after extraction was 62.5 g, while the residual 113.5 g was washed several times, and dried at room temperature in open air and kept for adsorption studies. A part of the powder was characterized by Fourier transform infrared (FT-IR) to elucidate the functional groups.

#### Batch adsorption experiment

Individually stock standard solution of 1000 mg/l of  $Pb^{2+}$  and  $Fe^{2+}$  were prepared by dissolving an amount of lead chloride and ferrous chloride in 1000 ml of DI water. Different concentrations (1, 5, 10, 20, 40, 50, 60, 80, 100 mg/l) were prepared by dilution of the stock solution with DI water. All batch adsorption experiments were performed on a mechanical shaker with a shaking speed of 160 rpm. To study the effect of adsorption time, 2 g of moringa seeds powder was agitated with 50 ml of 100 mg/l of  $Pb^{2+}$  and  $Fe^{2+}$  solutions at interval times (10, 20, 30, 40, 50, 60, 70, 80, 90, 120, 150 and 180 min.). The initial pH values of the  $Pb^{2+}$  and  $Fe^{2+}$  solutions were adjusted by adding 1:1 HCl and 1 % NaOH solutions. After each adsorption processes, the solution was filtrated, and the supernatant was immediately analyzed by inductive coupled plasma Mass Spectrometry (ICP-MS). The adsorption capacity was calculated according to the following equation;

$$q = \frac{(C_i - C_f)V}{m}$$

The removal % was calculated as follows;

$$\% = \frac{(C_i - C_f)}{C_i} \times 100$$

Where  $q$  is the adsorption capacity (mg/g),  $C_i$  and  $C_f$  are the initial and the final metal ion concentrations (mg/L),  $V$  is the volume of the adsorbate solution (L), and  $m$  is the mass of adsorbent (g).

**Results and Discussions**

**Groundwater chemistry:**

The classification of the Pleistocene water samples in the study area based on TDS values according to Freeze and Cherry, 1979 classification reflected that 80% of samples are fresh water and 20% of samples are brackish, (Table, 1). TDS distribution map (Fig. 3) shows that spatial changes of TDS values may be due to aquifer lithology, the presence of the lower Pliocene clay minerals.

**Table 1:** Groundwater type based on TDS values in El-Sadat area.

Parameter	Classification	Water type/ suitability	No. of groundwater samples	%
TDS (mg/l) (Freeze and Cherry 1979)	1000	Fresh	20	80
	1000 - 10000	Brackish	5	20
	10000 - 100000	Saline	0	0
	> 100000	Brine	0	0

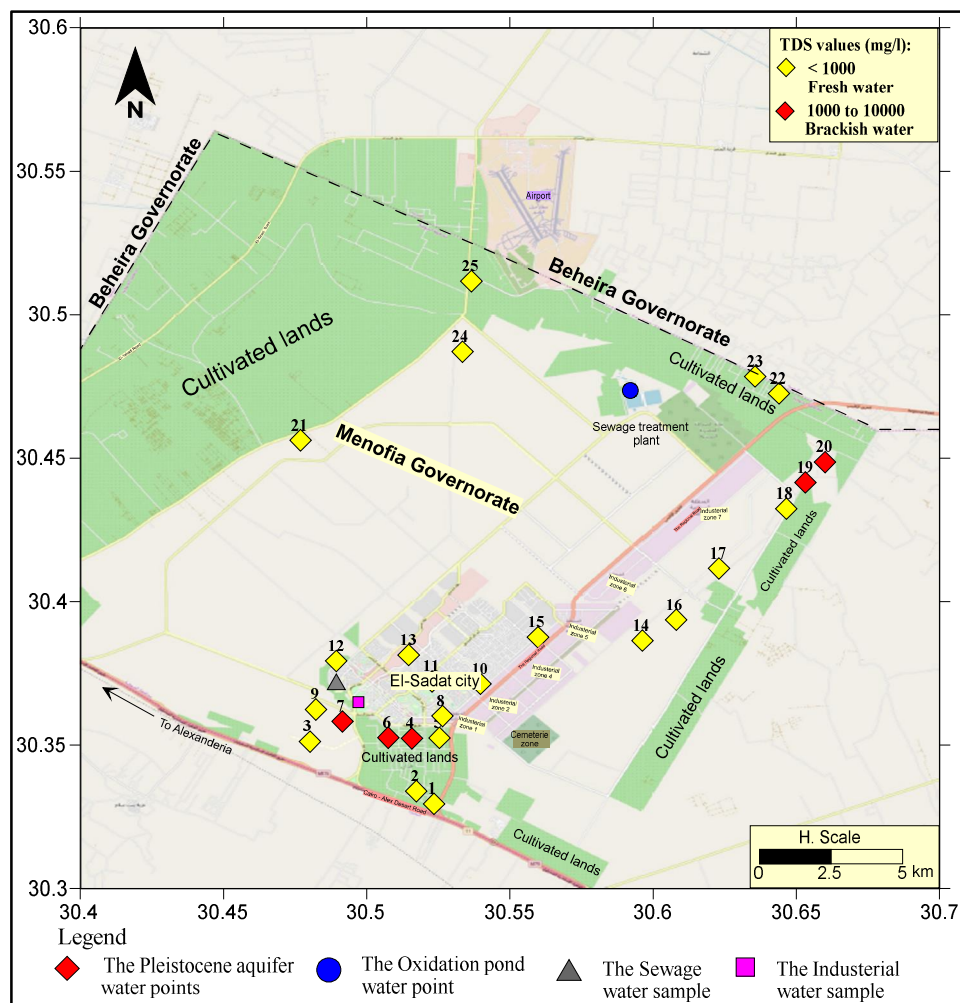


**Fig. 3:** Spatial distribution of the Pleistocene water samples based on TDS values according to Freeze and Cherry, 1979 classification in El-Sadat area.

The presence of Cl/Br mass ratio expected from unpolluted marine water is equal to  $650 \pm 4$  and leachate from septic tank = 450 (Alcalá and Custodio, 2008) which is greater than the values of the Pleistocene groundwater, the values are ranges from 42.4 to 164.5, the nitrate source of groundwater contamination is from seepage of runoff from fertilizer use, leaking from septic tanks, sewage and

erosion of natural deposits (WHO,1993). The  $\text{NO}_3/\text{Cl}$  mass ratio values of the Pleistocene groundwater (Table, 2) ranges from 0.03 to 1.02 shows greater values than that of excepted from marine source  $> 0.0002$  (McArthur *et al.*, 2012),  $\text{SO}_4/\text{Cl}$  mass ratio of all the Pleistocene water samples are greater than excepted from marine source  $> 0.14$ , the values ranges between 0.41 and 2, and two Pleistocene water samples only shows  $\text{NH}_4/\text{Cl}$  mass value greater than that expected from the marine source ( $>0.07$ ) (McArthur *et al.*, 2012) the previous results may be indicates that the groundwater contamination is from anthropogenic activity source.

The nitrate pollution index (NPI) values (Table, 2) shows that 72% of the Pleistocene water samples are clean (unpolluted), 20 of samples are light polluted and 8% of samples are moderate polluted where the oxidation pond water sample is moderate polluted, industrial sewage is light polluted and domestic sewage water is moderate polluted. The spatial distribution of the NPI values (Fig. 4) presented three major zones varies from unpolluted zone in the north west to moderate polluted zone in the south east (cultivated lands) may be indicated that the nitrate contamination source is from agricultural activities, due to nitrification of synthetic fertilizers and soil organic nitrogen (Ahmed *et al.*, 2011).

**Table 2:** Chemical compositions (Major and minor constituents) of the water samples in El-Sadat area

No.	pH	EC	TDS	Na	K	$\text{SO}_4$	Cl	$\text{NO}_3$
1	8.36	485	278	57	2.2	33.2	42.4	43.2
2	8.25	1522	820	182	4.4	169.4	311.1	9.9
3	8.14	788	418	106	2.2	91.3	124.4	6.6
4	7.92	3751	2060	418	9.4	550.0	777.7	38.2
5	8.47	1553	811	176	5.5	174.1	299.8	49.1
6	8.25	2127	1137	231	7.7	260.8	435.5	15.4
7	8.36	2048	1194	341	3.3	398.2	333.7	24.1
8	8.03	1057	587	110	4.4	155.9	178.2	17.6
9	8.25	1285	670	149	4.4	145.3	237.6	6.2
10	7.92	510	260	46	3.3	66.0	50.9	15.4
11	8.03	1101	626	114	4.4	175.6	181.0	12.1
12	8.03	1098	553	101	3.3	104.9	212.1	15.2
13	8.14	606	308	64	4.4	74.8	67.9	20.9
14	8.14	411	212	29	3.3	52.8	36.5	4.5
15	8.14	541	268	46	3.3	66.0	56.6	8.1
16	8.03	397	191	26	3.3	40.2	33.9	30.9
17	8.03	472	268	37	3.3	84.9	42.4	11.0
18	7.48	1032	598	44	5.5	178.5	189.5	19.9
19	7.59	2091	1277	176	7.7	447.4	373.3	20.8
20	7.81	2037	1251	154	7.7	462.0	362.0	4.6
21	8.14	452	270	57	3.3	87.3	42.4	15.1
22	7.59	997	564	92	5.5	176.0	147.6	6.7
23	7.92	429	248	22	4.4	66.0	50.8	9.6
24	7.92	421	240	40	3.3	63.8	46.5	12.5
25	8.25	480	276	51	3.3	66.0	63.9	3.1
O.P	6.60	4380	2199	360	30	350.0	848.4	44.4
D.S	6.80	1220	591	120	17	186.8	102.8	9.4
I.S	6.60	1547	768	144	16	190.0	216.0	34.0

**Table 2:** Continued

No.	$\text{NH}_4$	Br	Cl/Br	Na/K	$\text{NO}_3/\text{Cl}$	$\text{NH}_4/\text{Cl}$	$\text{SO}_4/\text{Cl}$	NPI
1	1.0	0.847	50.08	26.00	1.02	0.025	0.78	1.16
2	0.9	3.30	94.27	41.25	0.03	0.003	0.54	-0.505
3	0.1	1.43	87.02	48.00	0.05	0.001	0.73	-0.67
4	0.1	6.49	119.83	44.43	0.05	0.001	0.71	0.91
5	0.1	3.19	93.97	32.00	0.16	0.001	0.58	1.455
6	0.2	4.73	92.07	30.00	0.04	0.001	0.60	-0.23

7	0.1	3.63	91.93	103.33	0.07	0.001	1.19	0.205
8	3.2	1.32	134.97	25.00	0.10	0.018	0.87	-0.12
9	0.1	3.08	77.13	33.75	0.03	0.001	0.61	-0.69
10	7.8	0.57	88.99	14.00	0.30	0.153	1.30	-0.23
11	6.3	1.10	164.54	26.00	0.07	0.035	0.97	-0.395
12	0.2	1.54	137.73	30.67	0.07	0.001	0.49	-0.24
13	0.0	0.56	120.98	14.50	0.31	0.001	1.10	0.045
14	2.0	0.52	70.64	8.67	0.12	0.054	1.45	-0.775
15	0.1	0.67	84.29	14.00	0.14	0.002	1.17	-0.595
16	1.4	0.43	79.11	8.00	0.91	0.042	1.19	0.545
17	7.7	0.42	101.48	11.33	0.26	0.182	2.00	-0.45
18	3.3	1.54	123.04	8.00	0.11	0.017	0.94	-0.005
19	3.0	2.97	125.69	22.86	0.06	0.008	1.20	0.04
20	4.1	3.19	113.48	20.00	0.01	0.011	1.28	-0.77
21	4.6	0.35	120.51	17.33	0.36	0.109	2.06	-0.245
22	1.0	1.54	95.86	16.80	0.05	0.007	1.19	-0.665
23	1.1	0.48	105.00	5.00	0.19	0.022	1.30	-0.52
24	5.7	0.31	151.07	12.00	0.27	0.123	1.37	-0.375
25	2.3	0.50	129.11	15.33	0.05	0.036	1.03	-0.845
O.P	44.7	20	42.42	12.00	0.05	0.05	0.41	1.22
D.S	61	1.6	64.27	7.06	0.09	0.59	1.82	-0.53
I.S	0.06	2.5	86.38	9.00	0.16	0.00	0.88	0.7

O.P: Oxidation Pond water sample      D.S: Domestic Sewage water sample      I.S: Industrial Sewage water sample

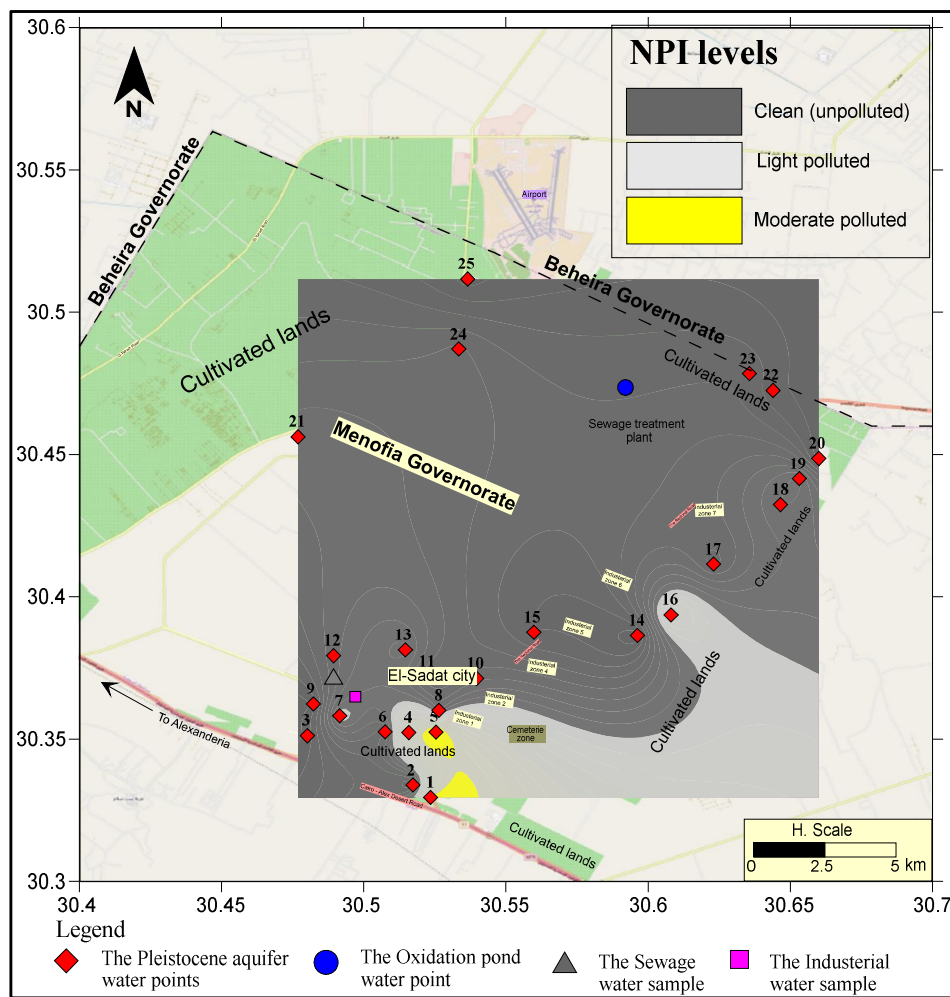


Fig. 4: Spatial distribution of the NPI values for the Pleistocene water samples.

Hierarchical cluster analysis is a multivariate statistical approach using for groundwater samples classification according to hydrochemical characteristics, the dendrograms were constructed by using the hydrochemical ratios ( $\text{NO}_3/\text{Cl}$ ,  $\text{NH}_4/\text{Cl}$ ,  $\text{SO}_4/\text{Cl}$ ,  $\text{Cl}/\text{Br}$  and  $\text{Na}/\text{K}$ ), PH, TDS, and heavy metal pollution index (HPI), finally, this correlation confirm that the hydrochemical ratios and the HPI represents the groundwater quality criteria. The R-mode dendrogram (Fig. 5). From R-mode dendrogram of the groundwater indicate that the parameters like hydrochemical ratios ( $\text{NO}_3/\text{Cl}$ ,  $\text{NH}_4/\text{Cl}$ ,  $\text{SO}_4/\text{Cl}$ ,  $\text{Cl}/\text{Br}$  and  $\text{Na}/\text{K}$ ), PH, heavy metal pollution index (HPI) show a close association. The Q-mode dendrogram reflects that the samples Nos., 2, 5, 8, 9, 11, 12, 18 and 22 are closely associated with the sewage contamination source (industrial and domestic sewage) reflected the impact of these sources on the Pleistocene groundwater closed to El-Sadat city and its industrial zones.

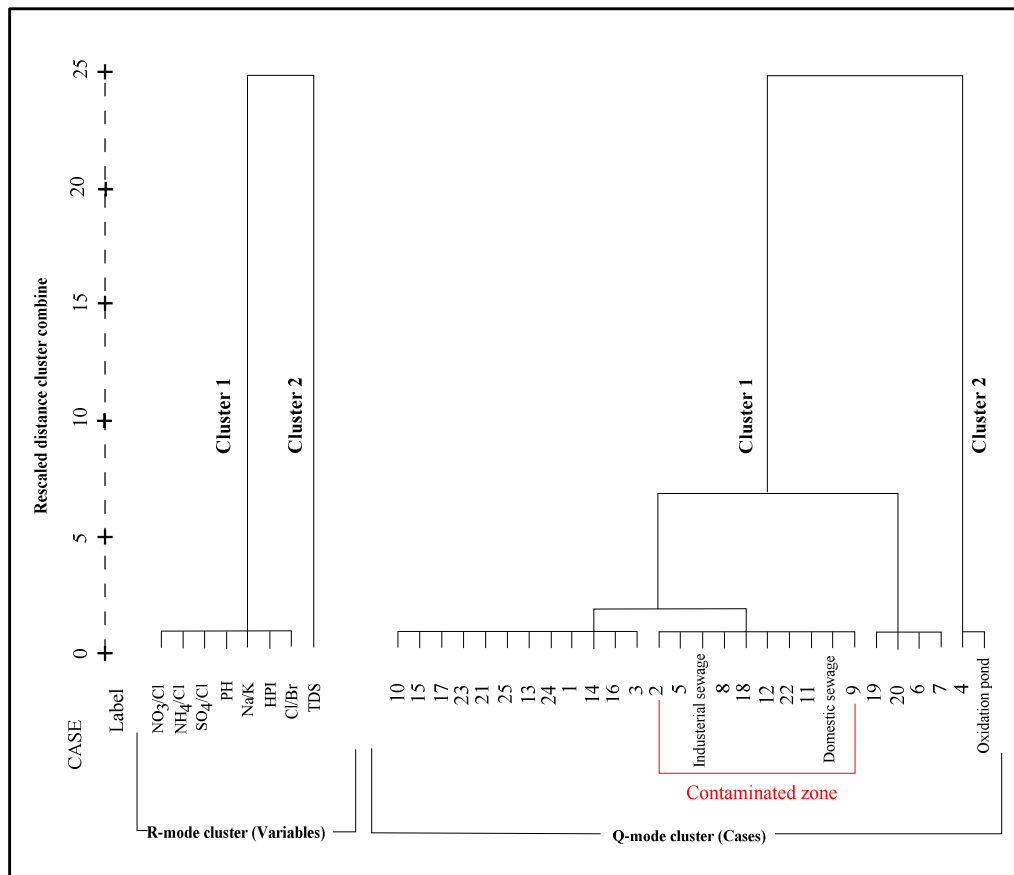


Fig. 5: Dendrogram (R-mode and Q-mode) for the water samples in El-Sadat area.

Ten heavy metals were analyzed in water samples in order to evaluate the quality of water resources in the study area; significance of the presence of heavy metals has been considered in framing the criteria for recommended limits in drinking water (Egy., 2007; WHO., 2006; US EPA., 2014).

From the chemical analysis of the heavy metals (Table, 3) reflects that the all the groundwater samples recorded low values less than the maximum contaminant level in respect to  $\text{Al}^{3+}$ ,  $\text{B}^{3+}$ ,  $\text{Cd}^{3+}$ ,  $\text{Cr}^{2+}$ ,  $\text{Cu}^{2+}$ ,  $\text{Ni}^{2+}$ , and  $\text{Zn}^{2+}$ . 24% of the groundwater samples are contaminated in respect to  $\text{Fe}^{2+}$  and  $\text{Mn}^{2+}$ , high local concentrations (6 samples) exceeded Iron and manganese permissible limits may be related to wastewater leakage from urbanization, industrial, and agricultural practices as well as aquifer lithology due to presence of iron oxide coating sand grains of the Pleistocene aquifer sediments (Awad *et al.*, 2015) and all the groundwater samples are contaminated in respect to  $\text{Pb}^{2+}$ . The surface water samples reflected that the oxidation pond is contaminated in respect to  $\text{Al}^{3+}$  and  $\text{Pb}^{2+}$ , the sewage sample is contaminated in respect to  $\text{Al}^{3+}$ , Fe and  $\text{Pb}^{2+}$  and the industrial sewage sample is contaminated in respect to  $\text{Pb}^{2+}$ . The overall quality of groundwater, HPI based on 10 metals was calculated according to the values in Table 2. HPI of groundwater samples ranges between 61 and 102 reflects that 36% of

groundwater samples are classified as poor samples, 60% are classified as very poor and 4% of samples are unsuitable samples. HPI of surface water samples ranges between 61 and 79 reflected that the sewages samples are classified as poor samples and the oxidation pond is classified as very poor sample (Table 3). The distribution map of HPI values (Fig. 6) reflects the increasing of the HPI values towards the south of the study area closed to the agricultural and industrial activities zones may be indicated that the heavy metal pollution source is from the anthropogenic activities (agricultural and industrial).

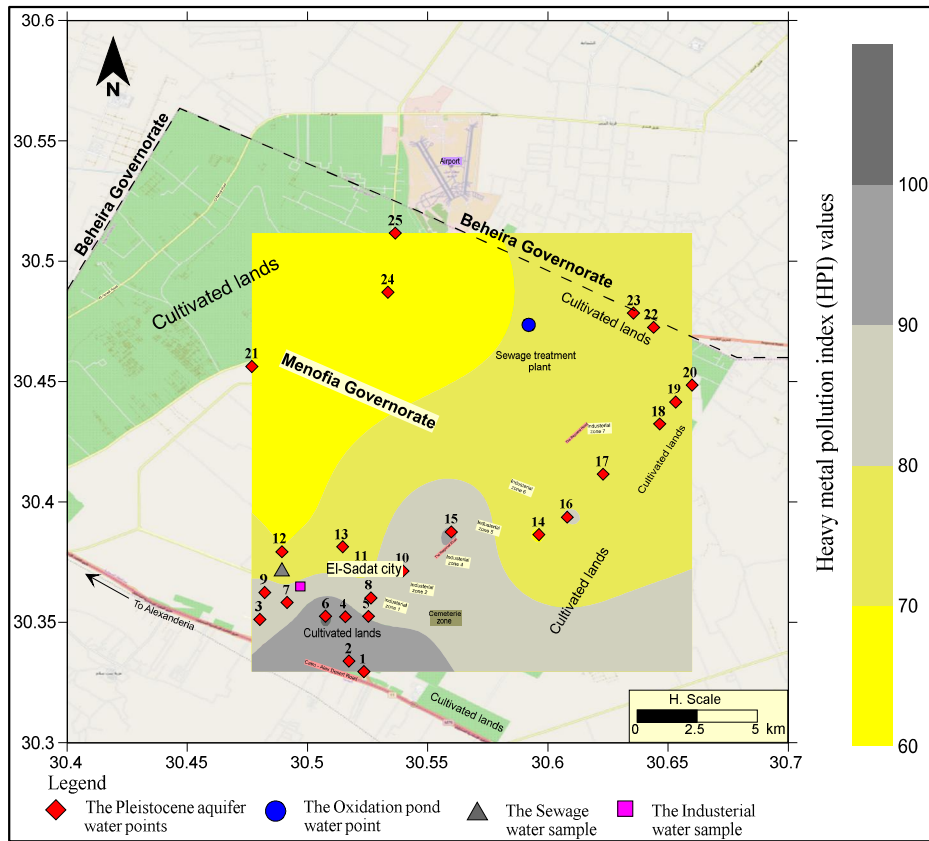


Fig. 6: Spatial distributions of the Pleistocene water samples based on HPI values in El-Sadat area.

Table 3: Chemical compositions of (trace and heavy metals) and Heavy metals pollution index (HPI) of the water samples in El-Sadat area

No	Al	B	Cd	Cr	Cu	Fe
1	<0.04	0.231	<0.0009	<0.01	<0.01	<0.03
2	<0.04	0.283	<0.0009	<0.01	<0.01	<0.03
3	<0.04	0.246	<0.0009	<0.01	<0.01	<0.03
4	<0.04	0.682	<0.0009	<0.01	<0.01	0.1364
5	<0.04	0.310	<0.0009	<0.01	<0.01	<0.03
6	<0.04	0.304	<0.0009	<0.01	<0.01	<b>0.4224</b>
7	<0.04	0.344	<0.0009	<0.01	<0.01	<0.03
8	<0.04	0.268	<0.0009	<0.01	<0.01	<0.03
9	<0.04	0.280	<0.0009	<0.01	<0.01	<b>0.3521</b>
10	<0.04	0.241	<0.0009	<0.01	<0.01	<0.03
11	<0.04	0.288	<0.0009	<0.01	<0.01	<0.03
12	<0.04	0.161	<0.0009	<0.01	<0.01	0.1602
13	<0.04	0.202	<0.0009	<0.01	<0.01	<0.03
14	<0.04	0.112	<0.0009	<0.01	<0.01	<0.03
15	<0.04	0.233	<0.0009	<0.01	<0.01	<b>1.098</b>
16	<0.04	0.103	<0.0009	<0.01	<0.01	<0.03
17	<0.04	0.144	<0.0009	<0.01	<0.01	<0.03
18	<0.04	0.138	<0.0009	<0.01	<0.01	<0.03

19	<0.04	0.315	<0.0009	<0.01	<0.01	<0.03
20	<0.04	0.280	<0.0009	<0.01	<0.01	0.1102
21	<0.04	0.105	<0.0009	<0.01	<0.01	<0.03
22	<0.04	0.166	<0.0009	<0.01	<0.01	<b>0.375</b>
23	<0.04	0.097	<0.0009	<0.01	<0.01	<b>0.377</b>
24	<0.04	0.091	<0.0009	<0.01	<0.01	<0.03
25	<0.04	0.109	<0.0009	<0.01	<0.01	<b>1.390</b>
O.P	<b>0.2238</b>	0.435	<0.0009	<0.01	<0.01	0.231
D.S	0.2047	0.165	<0.0009	<0.01	<0.01	<b>0.379</b>
I.S	<0.04	0.231	<0.0009	<0.01	<0.01	0.260

Table 3: Continued

No	Mn	Ni	Pb	Zn	HPI
1	<0.003	<0.002	<b>0.038</b>	<0.0006	95
2	<0.003	<0.002	<b>0.039</b>	0.0013	94
3	<0.003	<0.002	<b>0.031</b>	0.0013	87
4	<0.003	<0.002	<b>0.037</b>	<0.0006	94
5	<0.003	<0.002	<b>0.035</b>	0.0051	90
6	<b>0.450</b>	<0.002	<b>0.041</b>	0.0029	102
7	<0.003	<0.002	<b>0.031</b>	0.0251	82
8	<0.003	<0.002	<b>0.033</b>	0.0076	84
9	0.018	<0.002	<b>0.032</b>	0.4398	84
10	<0.003	<0.002	<b>0.034</b>	0.0052	88
11	<0.003	<0.002	<b>0.029</b>	0.0189	77
12	0.023	<0.002	<b>0.024</b>	0.0197	70
13	<0.003	<0.002	<b>0.026</b>	0.0097	74
14	<0.003	<0.002	<b>0.025</b>	0.1330	68
15	<0.003	<0.002	<b>0.034</b>	0.0975	91
16	<0.003	<0.002	<b>0.031</b>	0.0229	82
17	<0.003	<0.002	<b>0.027</b>	0.0035	72
18	0.024	<0.002	<b>0.030</b>	0.0041	78
19	<b>0.514</b>	<0.002	<b>0.025</b>	0.0120	71
20	<b>0.431</b>	<0.002	<b>0.028</b>	0.0271	78
21	<0.003	<0.002	<b>0.023</b>	0.0073	66
22	<b>0.511</b>	<0.002	<b>0.027</b>	0.0007	75
23	<b>0.480</b>	<0.002	<b>0.025</b>	0.0024	75
24	0.088	<0.002	<b>0.021</b>	<0.0006	61
25	<b>0.427</b>	<0.002	<b>0.023</b>	0.0035	69
O.P	0.175	<0.002	<b>0.029</b>	0.0261	79
D.S	0.066	<0.002	<b>0.019</b>	0.1657	61
I.S	0.096	<0.002	<b>0.021</b>	0.0338	64

O.P: Oxidation pond water sample D.S: Domestic sewage water sample I.S: Industrial sewage water sample  
 Bold font values mean more than the maximum contaminant level

### Adsorption of Fe<sup>2+</sup> and Pb<sup>2+</sup> ions using moringa seeds

ATFTIR spectrum of grinded moringa seeds powder was measured to detect the functional groups that are responsible of heavy metal adsorption. (Fig. 7) reveals a broad band around 3330 cm<sup>-1</sup> that is attributed to stretching of hydroxyl group characterized to proteins, fatty acids, and carbohydrate units (Irene, 2016). The peaks at 2921 and 2852cm<sup>-1</sup> corresponds to asymmetric and symmetric stretching CH<sub>2</sub> groups. The bands at 1770 and 1648 cm<sup>-1</sup> represent the stretching of the carbonyl group that is the main group of proteins and lipids present in the moringa seed. The amino groups of the peptide are represented by the stretching bands of 1507 and 1521 cm<sup>-1</sup>. All of these moringa characteristic groups (Hydroxyl, carbonyl and amine) consider the active sites of heavy metal adsorption.

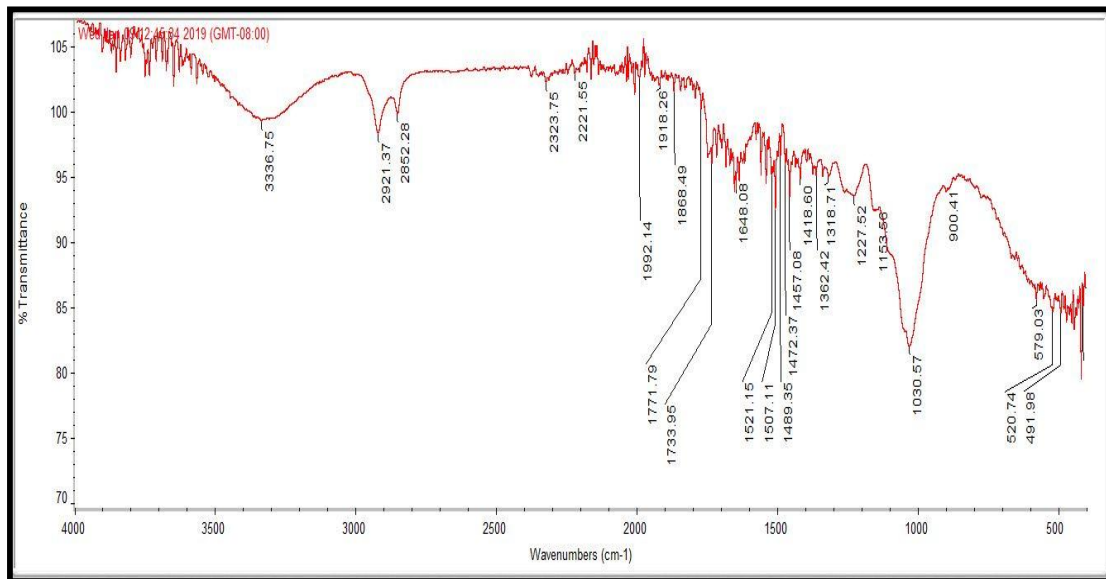


Fig. 7: Attenuated Total Reflectance FT-IR of Moringa seeds

Different factors affect the adsorption efficiency of the moringa seeds for  $Fe^{2+}$  and  $Pb^{2+}$  ions have been investigating. Fig. 8 shows the effect of moringa seed dose onto the removal efficiency and adsorption capacity ( $q$ ) of  $Fe^{2+}$  and  $Pb^{2+}$  ions. The initial concentrations of both ion solutions were 100 mg/l, pH 3.5 at 25 °C, while the moringa dose varied between 0.5 and 15 g/l. The figure reveals that the removal efficiency of the both ions increased up to 98 % as the adsorbent dose increased from 0.5 to 15 g/l. While the optimum dose regard to the higher adsorption capacity is less than 2 g/l. This increase of adsorption is due to increasing the active sites (hydroxyl, amine, and carbonyl functional groups) onto the moringa surfaces as a function of adsorbent dose increase. The steady state of adsorption of both ions was observed at 10 g/l. pH of the adsorbate solution plays an important role during the adsorption process due to protonation or de-protonation of the functional groups of the moringa seed. Fig. 9 shows the effect of pH on the removal efficiency of  $Fe^{2+}$  and  $Pb^{2+}$  ions using a constant dose (5 g/l) of the moringa seeds and constant initial ion solutions concentrations (100 mg/l). From the figure, the maximum removal efficiency is shown at slightly acidic medium (pH 5). At higher pH de-protonation of the moringa seeds functional groups might occurs, which increase the electrostatic interaction of the positively charged ions onto the surfaces.

Adsorption isotherms are important criteria in optimizing the use of adsorbents as they describe the nature of interaction between adsorbate and adsorbent. Thus, analysis of experimentally obtained equilibrium data by either theoretical or empirical equations is useful for practical design and operation of adsorption systems. The Langmuir and Freundlich adsorption isotherms were applied to each metal under study. The adsorption mechanism and experimental date of  $Fe^{2+}$  and  $Pb^{2+}$  ions onto the surfaces of moringa seeds powder were investigated by using isotherm models of Langmuir and Freundlich, equations 1 and 2 respectively.

$$\frac{C_e}{q_e} = \frac{1}{K_L q_m} = \frac{C_e}{q_m} \dots\dots\dots (1)$$

$$\text{Log } q_e = \ln KF + (1/n) \text{ log } C_e \dots\dots\dots (2)$$

Where  $C_e$  is the equilibrium concentration of the adsorbed ions (mg/l),  $q_e$  and  $q_m$  are the adsorption amount at equilibrium (mg/g) and maximum adsorption capacity (mg/g), respectively,  $K_L$  is the Langmuir constant (L/mg). The values of  $K_L$  and  $q_m$  can be obtained from the intercept and slope of plotting  $C_e/q_e$  versus  $C_e$  (Fig. 10A).  $K_F$  and  $1/n$  are the empirical Freundlich constant (mg/g) and Freundlich exponent, respectively. The values of  $K_F$  and  $1/n$  can be expressed from the intercept and slope of plotting  $\text{Log } q_e$  versus  $\text{Log } q_c$  (Fig. 10B).

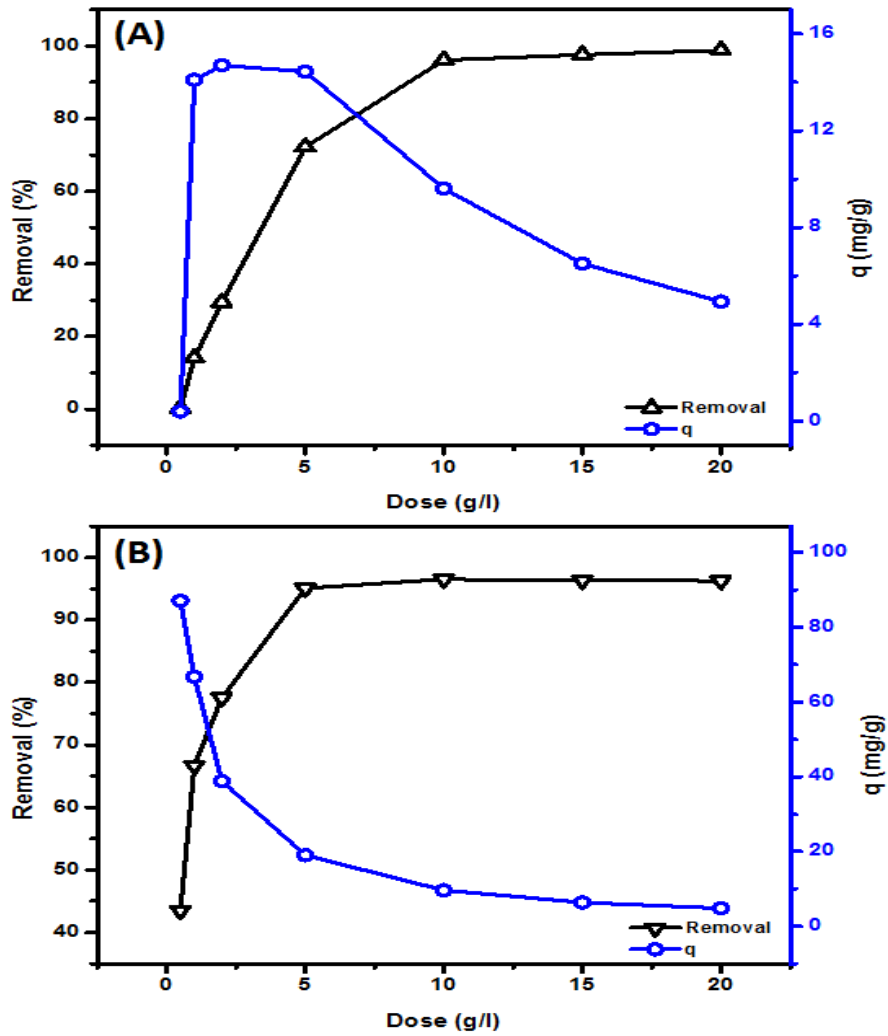


Fig. 8: The removal efficiency and adsorption capacity of moringa seeds as a function of dose of A) Fe<sup>2+</sup> and B) Pb<sup>2+</sup>

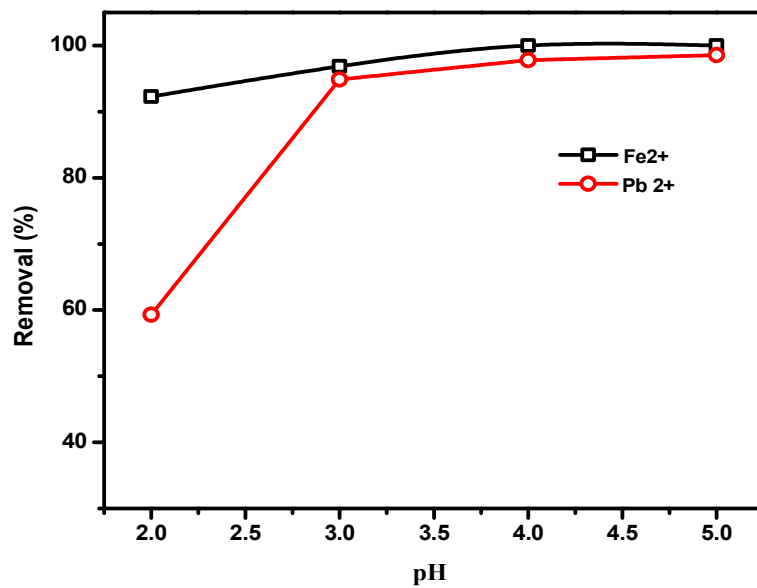


Fig. 9: Effect of pH of the adsorption solution onto the removal efficiency of moringa seeds for removal of Fe<sup>2+</sup> and Pb<sup>2+</sup>

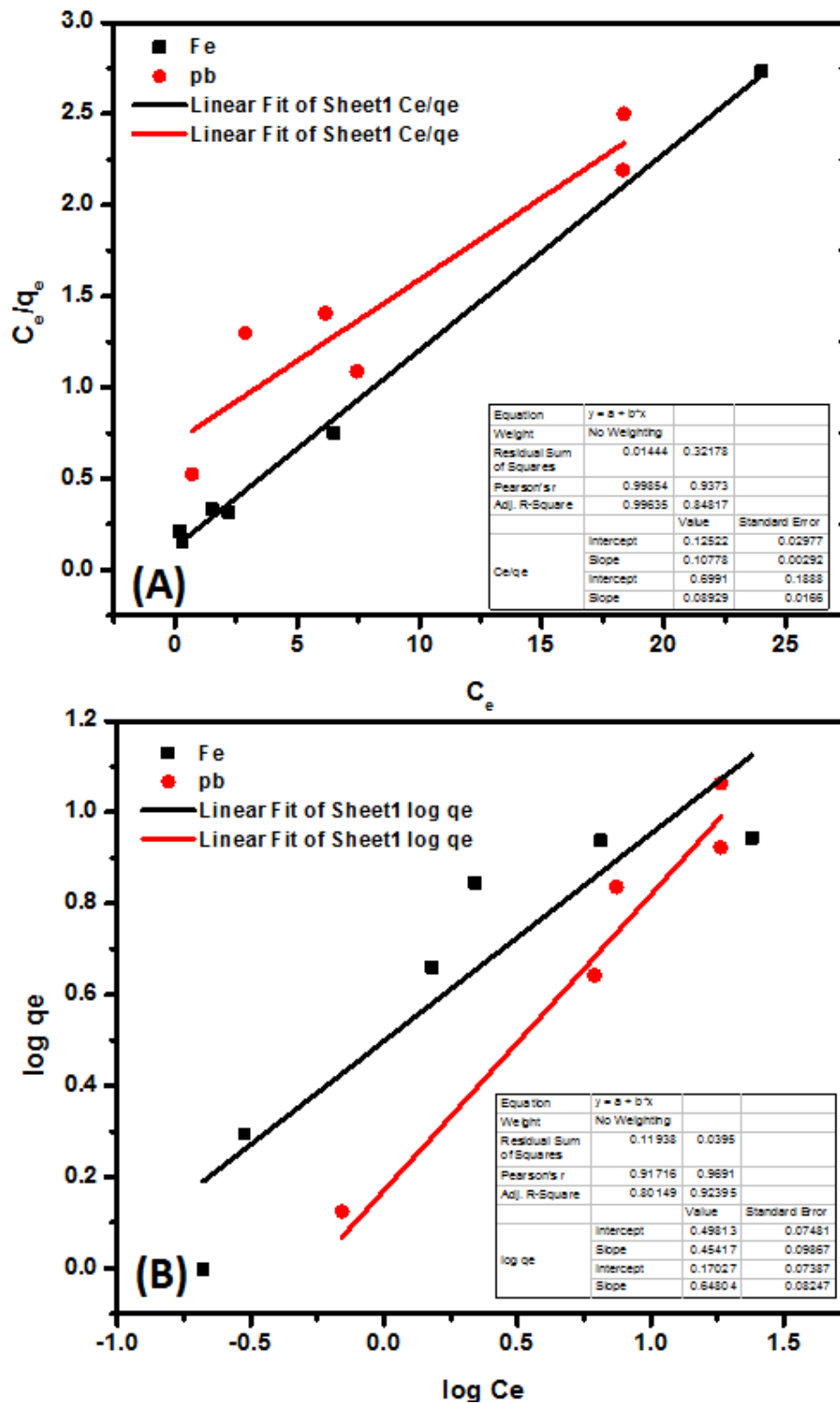


Fig. 10: A) Langmuir isotherm model and B) Freundlich isotherm model of  $Fe^{2+}$  and  $Pb^{2+}$  onto moringa seeds

Based on the regression correlation coefficient ( $R^2$ ) values, the adsorption of  $Fe^{2+}$  fits better to Freundlich model than the Langmuir, and vice versa in case of  $Pb^{2+}$ . However, Langmuir isotherm model suggests adsorption of ions onto the adsorbent surface as a monolayer excluding any interaction between the adsorbed molecules. While, Freundlich adsorption isotherm describes that absorption process occurs on an energetically heterogeneous surface of the adsorbent. Table 4 shows that both the adsorption intensity ( $k_F$ ) and multilayer adsorption capacity ( $n_F$ ) values of  $Fe^{2+}$  are higher than that of  $Pb^{2+}$ . This indicates that the adsorption of  $Fe^{2+}$  is a heterogeneous multilayer formation process, while  $Pb^{2+}$  adsorption is less favoured by this process. To predict if the adsorption process is favorable or unfavorable, the equilibrium parameter ( $R_L$ ) was calculated according to the following equation.

$$R_L = \frac{1}{1 + K_L \cdot C_f}$$

Where  $K_L$  is the Langmuir constant (l/mg) and  $C_f$  is the final ion concentration (mg/l) in the solution. If  $R_L > 1$  the isotherm is unfavorable, whereas if  $R_L < 1$  the isotherm is favorable. The calculated  $R_L$  values at different concentrations were found to be less than unity indicating the adsorption of ions onto moringa seeds is favorable. In addition, from the data of Freundlich isotherm model it was found that  $1/n$  values (0.45 of  $Fe^{2+}$  and 0.64 of  $Pb^{2+}$ ) are less than unity, which indicates a favorable adsorption.

**Table 4:** Langmuir and Freundlich isotherm model parameters

Ion	Langmuir isotherm				Freundlich isotherm			
	$Q_{max}$	$K_L$	$R^2$	n	1/n	$R^2$	$K_F$	$R_L$
$Pb^{2+}$	11.19	0.12	0.87	1.54	0.648	0.93	-1.77	0.299
$Fe^{2+}$	9.27	0.86	0.99	2.2	0.454	0.84	-0.696	0.151

### Conclusion

Groundwater quality parameters clearly indicated the contamination source of the Pleistocene groundwater in El-Sadat city and its vicinities by some heavy metals. The total dissolved solids (TDS) values reflect that 80 % of the Pleistocene groundwater samples are fresh while the rest are brackish. The hydrochemical ratios ( $NO_3^-/Cl^-$ ,  $SO_4^{2-}/Cl^-$  and  $NH_4^+/Cl^-$ ), nitrate pollution index (NPI) and the statistical analysis revealed groundwater contamination by seepage from fertilizer use, leaking from septic tanks, sewage and erosion of natural deposits. The overall quality of groundwater, HPI based on 10 metals reflects that 36% of groundwater samples are classified as poor samples, 60% are classified as very poor and 4% of samples are unsuitable samples. HPI of surface water samples ranges between 61 and 79 reflected that the sewages samples are classified as poor samples and the oxidation pond is classified as very poor sample. In terms of heavy metal ions, 24% of the groundwater samples are contaminated in respect to  $Fe^{2+}$  high local concentrations (6 samples) exceeded Iron permissible limits may be related to wastewater leakage from urbanization, industrial, and agricultural practices as well as aquifer lithology due to presence of iron oxide coating sand grains of the Pleistocene aquifer sediments, whereas all samples are contaminated by  $Pb^{2+}$ . Therefore, moringa seeds were used to adsorb or remove these toxic ions from water. It was found that the removal efficiency of the both ions improved up to 98 % as the adsorbent dose increased from 0.5 to 15 g/l. The adsorption of  $Fe^{2+}$  was fitted better to Freundlich model than the Langmuir, and vice versa in case of  $Pb^{2+}$ . The above results confirm that moringa seeds can be used as an effective adsorbate for the heavy metals from groundwater, which have some high concentrations of  $Fe^{2+}$ . For example, the groundwater sample (No. 25, Table 3) containing 1.39 mg/l of  $Fe^{2+}$ , more than the permissible limit, was found to be free of  $Fe^{2+}$  after batch adsorption experiment by moringa seeds.

### References

- Abd El-Baki, A.A., 1983. Hydrogeological and hydrogeochemical studies in the area west of Rosetta branch and south of El Nasr canal. Ph.D. Thesis, Fac. Sci., Ain Shams University.  
 Abdel-Shafy, H.I. and M.S., Mansour, 2013. Overview on water reuse in Egypt: Present and Future. Sustainable Sanitation Practice, 14: 17-25.

- Agrama, A.A., and E.A. El-Sayed, 2013. Assessing and mapping water quality (Case study: Western Delta-Egypt). *I.W.T.J.* 3: 158-169.
- Ahmed, M. A., S. G. A. Samie, and H. M. El-Maghrabi, 2011. Recharge and contamination sources of shallow and deep groundwater of pleistocene aquifer in El-Sadat industrial city: isotope and hydrochemical approaches. *Environmental Earth Sciences*, 62(4): 751–768.
- Alcalá, F. J., and E. Custodio, 2008. Using the Cl/Br ratio as a tracer to identify the origin of salinity in aquifers in Spain and Portugal *J. Hydrol.* 359:189–207.
- Alinnor, J., 2007. Adsorption of heavy metal ions from aqueous solution by fly ash. *Fuel*, 86(5-6) 853–857.
- Al-Kilany, S.M., 2001. A new geoelectrical studies on groundwater aquifer, El-Sadat area and its vicinities Egypt. Dissertation, Menoufiya University, Egypt.
- Allam, A.R., E. Saaf, and M.A. Dawoud, 2003. Desalination of brackish groundwater in Egypt. *Desalination*, 152: 19-26.
- Annadurai, G., R. S. Juang, and D. J. Lee, 2003. Adsorption of heavy metals from water using banana and orange peels. *Water Science and Technology*, 47(1): 185–190.
- Awad S.R., M.A. El Fakharany, and N.M. Hagra, 2015. Environmental Impact on Water Resources at the Northwestern Part of the Nile Delta, Egypt. *Journal of American Science*, 11:(11).
- CONOCO, 1987. Geological map of Egypt, scale 1:500,000. Map sheet no NH36NW, Cairo, Egypt
- Egy. 2016. Water quality guidelines for human drinking, domestic and laundry uses, Egypt, decree No. 458/2007 (in Arabic).
- El-Sayed, S.A., 1999. Hydrogeological and isotope assessment of groundwater in Wadi El-Natron and Sadat City, Egypt. Dissertation, Ain Shams University, Egypt.
- Freeze, R.A, and J.A. Cherry, 1979. *Groundwater*. Prentice Hall Inc, New Jersey.
- Fu, F., and Q. Wang, 2011. Removal of heavy metal ions from wastewaters: a review. *Journal of Environmental Management*, 92(3): 407–418.
- Ghaly, S.S., 2001, Environmental Impact of Artificial Recharge on Groundwater In Bustan Extension Area. Master thesis, Faculty of Engineering- Ain Shams University, Egypt.
- Glenda, M.H. and D.J. Gregory, 1996. Home Drinking Water Treatment Systems. *Water Quality and Waste Management*. North Carolina Cooperative Extension Services. HE- 419.
- Gupta, V.K., A. Rastogi and A. Nayak, 2010. Adsorption studies on the removal of hexavalent chromium from aqueous solution using a low cost fertilizer industry waste material. *Journal of Colloid and Interface Science*. 342(1): 135-141.
- Horton, R.K., 1965. An index number system for rating water quality. *J Water Pollut Control Fed* 37(3):300–306.
- Irene W. M., O. Veronica, and N. Florence, 2016. Use of *Moringa oleifera* (Moringa) Seed Pods and *Sclerocarya birrea* (Morula) Nut Shells for Removal of Heavy Metals from Wastewater and Borehole Water. *Journal of Chemistry*, 13.
- Kenawy, A.A., U. Massoud, E.-S. A. Ragab, and H. M. El-Kosery, 2016. Investigation of the probable wastewater infiltration and its impact on groundwater quality by electrical resistivity tomography and hydrochemistry: a case study of the Pleistocene aquifer at El Sadat city, Egypt. *Environmental Earth Sciences*, 75 :( 3).
- McArthur, J.M., P.K. Sikdar, M.A. Hoque and U. Ghosal, 2012. Waste-water impacts on groundwater: Cl/Br ratios and implications for arsenic pollution of groundwater in the Bengal Basin and Red River Basin, Vietnam. *Science of the Total Environment* 437: 390– 402.
- McLay, C.D.A., Dragten, R., G. Sparling, , and N. Selvarajah, , 2001. Predicting groundwater nitrate concentrations in a region of mixed agricultural land use: a comparison of three approaches. *Environmental Pollution*, 115: 191-204, ISSN 0269-7491.
- Menco, 1990. Miser company for engineering and agricultural projects report.
- Mohan, S., P. Nithila and S. Reddy, 1996. Estimation of heavy metal in drinking water and development of heavy metal pollution index". *Environ. Sci. J Health A.*, 31(2):283.
- Najafabadi, H.H., 2015. Removal of Cu<sup>2+</sup>, Pb<sup>2+</sup> and Cr<sup>6+</sup> from aqueous solutions using a chitosan/graphene oxide composite nanofibrous adsorbent. *RSC Adv.*, 5(21): 16532-16539.
- Obuseng, V., N. Florence and K. Habauka, 2012. A study of the removal of heavy metals from aqueous solutions by *Moringa oleifera* seeds and amine-based ligand 1,4-bis[N,N-bis(2 picoyl)amino]butane. *Analytica Chimica Acta*, 730:87-92.

- Piedra, E., J. R. Álvarez, et al., 2015. Hexavalent chromium removal from chromium plating rinsing water with membrane technology. *Desalination and Water Treatment* 53(6): 1431-1439.
- Reddy, D.H.K., K. Seshaiyah, A.V.R. Reddy, M. M. Rao, and M.C. Wang, 2010. Biosorption of Pb<sup>2+</sup> from aqueous solutions by *Moringa oleifera* bark: equilibrium and kinetic studies. *Journal of Hazardous Materials*, 174: 831–838.
- Reddy, D.H.K., K. Seshaiyah, A.V.R. Reddy, and S.M. Leec, 2012. Optimization of Cd(II), Cu(II) and Ni(II) biosorption by chemically modified *Moringa oleifera* leaves powder. *Carbohydrate Polymers* 88, 1077–1086.
- Sharaky, A.M., S.A. Atta, A.S. El Hassanein, and K.M. Kallaf, 2007. Hydrogeochemistry of groundwater in the Western Nile Delta aquifers, Egypt. *Proceedings of the 2nd International Conference on the Geology of Tethys*, Cairo University, Egypt, 1-23.
- Singh, K. K., M. Talat, and S.H. Hasan, 2006. Removal of lead from aqueous solutions by agricultural waste maize bran. *Bioresource Technology*, 97(16): 2124–2130.
- Spalding, R.F. and M.E. Exner, 1993. Occurrence of nitrate in groundwater- a review. *Journal of Environmental Quality*, 22: 392-402..
- US EPA, 2014. Drinking Water Contaminants. Available from: <https://www.epa.gov/ground-water-and-drinking-water/table-regulated-drinking-water-contaminants>. Accessed on 1 July 2016.
- Veronica, O., N. Florence, and M.K. Habauka, 2012. A study of the removal of heavy metals from aqueous solutions by *Moringa oleifera* seeds and amine-based ligand 1,4-bis[N,N-bis(2-picoyl)amino]butane. *Analytica Chimica Acta* ,730: 87–92.
- WHO, 1993. World Health Organization guidelines for drinking water quality, vol. 1, 2nd edn, Recommendations, WHO, Geneva, 130.
- WHO, 2006. World Health Organization, MCLs., 2006. A compendium of drinking-water quality standards in the eastern Mediterranean region". World Health Organization Regional Office for the Eastern Mediterranean Regional Centre for Environmental Health Activities CEHA 2006.